Metabolism of Tac (IL2Rα): Physiology of Cell Surface Shedding and Renal Catabolism, and Suppression of Catabolism by Antibody Binding

By R.P. Junghans* and T.A. Waldmann‡

*From the *Division of Hematology-Oncology, Harvard Medical School, Biotherapeutics Development Lab, New England Deaconess Hospital, Boston, Massachusetts 02215; and the ‡Metabolism Branch, National Cancer Institute, National Institutes of Health, Bethesda, Maryland 20892*

Summary

The interleukin 2 receptor α (IL2Rα; CD25; Tac) is the prototypic model for soluble receptor studies. It exists in vivo as a transmembrane complete molecule (TM-Tac) on cell surfaces and as a truncated soluble form (sTac; sIL2Rα). sTac has been used as a serum marker of T cell activation in immune disorders and of tumor burden in Tac-expressing malignancies. In vivo, serum levels of all soluble proteins depend on the balance between production and catabolism, but little is known about the metabolic features of this class of molecules. We have developed a model for Tac metabolism that incorporates new insights in its production and catabolism. Tac was shed from the surface of malignant and activated human T cells with a modal half-life ($t_{1/2}$) of 2–6 h, but which was prolonged under certain circumstances. The rate of shedding is first order overall and nonsaturable over a two order of magnitude range of substrate (TM-Tac) expression. Once shed from cells, sTac is subject to catabolic activities in the host. In vivo studies in mice showed that 90% of sTac was catabolized by the kidney with a $t_{1/2}$ of 1 h and a filtration fraction of 0.11 relative to creatinine. The remaining 10% of catabolism was mediated by other tissues with a $t_{1/2}$ of 10 h. Approximately 1–3% of sTac is excreted intact as proteinuria with the remaining 97–99% catabolized to amino acids. Antibody to the receptor induced a marked delay in sTac catabolism by preventing filtration of the smaller protein through the renal glomerulus and additionally suppressing other nonrenal catabolic mechanisms. A discrepancy between the catabolic rates for Tac and anti-Tac in the same complex was interpreted as a previously unrecognized differential catabolic mechanism, suggesting features of the Brambell hypothesis and immunoglobulin G transport and catabolism, in which the antigen-in-complex in intracellular vesicles is relatively less protected from catabolism than the associated antibody. In light of the pivotal role played by the kidney in sTac catabolism and the impact of administered antibody, the serum concentration of Tac in the settings of renal dysfunction or antibody therapy is not a suitable surrogate of activated T cells or of the body burden of tumor. These results provide parameters for assessing soluble receptor–ligand interactions generally.

Cell surface receptors, adhesion molecules, and their shed soluble forms are increasingly the subject of biological and clinical investigations (1, 2). They are widely evaluated for diagnosis and prognosis in human disease (3), and as treatment targets or as therapeutic agents themselves (4, 5). The array of surface structures generating soluble forms is very large, tallied at 43 in a 1991 review (6), with further molecules described since that time. Yet there is little data on the generation, distribution, and pharmacology of soluble receptors in general.

The prototypic model for these receptors is the IL2R α chain. It was among the first to be recognized as having a soluble form, and has additionally been the subject of diverse laboratory and clinical investigations. The full IL2R plays a central role in lymphocyte activation and proliferation. It is comprised of at least three chains (α, β, γ), of which the α chain (IL2Rα; CD25), termed "Tac"[1] for T

[1] *Abbreviations used in his paper:* ATL, adult T cell leukemia; CEA, carcinoembryonic antigen; GFR, glomerular filtration rate; S, substrate surface TM-Tac; ss, steady state; sTac, soluble Tac; TM-Tac, transmembrane Tac; constants: k, Tac shedding rate constant; k_{met}, Tac metabolic rate constant; k_r, renal component of k_{met}; k_{nr}, nonrenal component of k_{met}; k_{ve}, k_{ev}, rate constants for vascular-to-extravascular and extravascular-to-vascular transport, respectively; q, Tac production rate constant; chemical species: A, anti-Tac; B, sTac; AB, monosaturated anti-Tac|Tac complex; AB_2, bisaturated anti-Tac|Tac_2 complex; A*, B*, AB*, A*B, A*B_2, AB_2*, radioactive components and their complexes.

 J. Exp. Med. © The Rockefeller University Press • 0022-1007/96/04/1587/16 $2.00
Volume 183 April 1996 1587–1602

activation antigen, is the most subject to regulation. Tac is not expressed on resting lymphocytes but is markedly upregulated with activation of T, B, and NK cells, and macrophages. As such, it has been used as a target for antibodies and other immunodirected therapies that selectively attack activated or malignant Tac-expressing cells while sparing the normal resting T cell repertoire (7). The expression of this molecule has been extensively investigated from the perspective of signaling events, promoter regulation, mRNA transcription, and protein synthesis (8).

The efferent part of Tac regulation—its catabolism—has been less well characterized. Similar to other shed molecules, little is known except that the soluble form of Tac (sTac) is generated in an active proteolytic process against the membrane-bound form (9). sTac levels have been suggested as surrogates of T cell activation in autoimmune and allograft settings and as a measure of tumor burden in Tac-expressing malignancies (10–15). sTac can accumulate to present a significant antigen load that binds administered antibody or IL2 toxin in anti-IL2R therapies, paralleling reports in antibody therapies directed against lymphomas expressing B cell idiotypes (16), melanomas and neuroendocrine tumors expressing gangliosides GD2 and GD3 (17, 18), and carcinomas expressing carcinoembryonic antigen (CEA) (19).

The serum level of sTac, as with all proteins, reflects a balance between the rate of synthesis and release from cells and the fractional rate of catabolism. To interpret soluble receptor levels in disease as a measure of cellular synthesis, one must equally understand the pathophysiological factors that regulate synthesis and that alter the catabolism of the protein. Similarly, the interaction with antibodies or other antireceptor molecules has the potential to perturb this in vivo balance. Accordingly, several aspects of the regulation of soluble receptor were examined. sTac production was measured from Tac-expressing human cells in culture to infer mechanisms of soluble receptor generation. Metabolic evaluations were performed in mice to derive pharmacokinetic parameters and to assess the role of the kidney in catabolism. Finally, reciprocal studies examined the impact of soluble receptor–antibody interactions on catabolism to anticipate the iatrogenic impact of such therapeutic interventions.

Materials and Methods

Cells and Cell Lines

Malignant cells from patients were harvested from blood on Ficoll-Hypaque. 2×10^6 cells were dispensed in 24-well plates in 2 ml RPMI 1640 + 5% human AB serum. Tac-expressing T cell line HuT102 was maintained in RPMI + 10% FCS.

Surface Tac (Transmembrane-Tac) and sTac

Viability was monitored by Trypan blue exclusion. Transmembrane (TM)-Tac was quantitated by ^{3}H-anti-Tac antibody (gift of R. Kozak, NIH, Bethesda, MD) binding modified from earlier methods (20). sTac was determined by ELISA (21) by a commercial laboratory (Hazleton Labs, Vienna, VA). The unit definition for sTac was ~3 pg or 0.13 fmol. One evaluation employed T cell activation data from Jacques et al. (22) in an assay closely parallel to our own.

Derivation of Tac Production Rate and Surface $t_{1/2}$

sTac (B) production is modeled as a first order process that is proportional to "substrate" surface TM-Tac expression (S):

$$dB/dt = kS \qquad \text{(Eq. 1)}$$

For fixed cell numbers and changing TM-Tac (primary malignant cells), solution yields:

$$\Delta B = {}^1/_2 k \Delta t (S + S_0) \qquad \text{(Eq. 2)}$$

Where TM-Tac is constant and cell number is changing (cell line HuT102), then

$$\Delta B = (k/c)\, S_0 (N_1 - N_0) \qquad \text{(Eq. 3)}$$

in which $c = ln\ (N_1/N_0)/\Delta t$. Where cell number and Tac/cell were varying (activated T cells), these methods were combined in a numerical solution (not shown).

Proteins and Radiolabeling

Recombinant human sTac (gift of J. Hakimi, Hoffmann-La Roche, Nutley, NJ) was >95% pure by HPLC and SDS-PAGE (not shown). Nonspecific murine antibody UPC (IgG2a, κ) was obtained from Cappell Laboratories (Cochranville, PA). Proteins were labeled with ^{131}I or ^{125}I to ~1–3 μCi/μg as described (20). Antibody bindability was assayed as described (20).

Mice

Nu/nu mice (Charles River Laboratories, Wilmington, MA) at 12–16 wk of age maintained on thyroid-blocking doses of KI were injected with radioproteins by tail vein or intraperitoneally in 0.2 ml of 1% BSA in PBS. Other animals were administered radioactivity in continuous infusions with 7-d microosmotic pumps (Alzet, Palo Alto, CA) implanted subcutaneously.

Assay of Protein Survival

For rapidly catabolized proteins, or with any protein in nephrectomized or ureter-ligated animals that cannot eliminate catabolic products, it is essential to assay protein-bound radioactivity instead of total radioactivity for pharmacokinetics. Methods were modified from Wochner et al. (23). Blood samples were collected in heparinized glass capillaries via tail vein, counted, and corrected for protein-bound counts by TCA precipitation or by exclusion chromatography of representative samples. For whole body catabolism, carcasses were individually homogenized and aliquots TCA-precipitated and processed.

Pharmacokinetic Modeling

Blood die-away curves of protein-associated counts were analyzed as two compartment models (Schema 1) using numerical integration by pcNONLIN 4.0 (SCI Software, Lexington, KY), except as noted. For nephrectomized or ureter-ligated animals, the gradual impact of uremia made it possible only to do α-phase modeling, approximated as a first order system over the first 4–8 h

of the assay. Nonstandard nomenclature is used to avoid confusion with other constants in the exposition.

Schema 1.

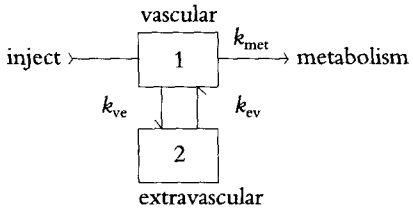

Relation of Renal Function to sTac Levels

sTac (B) concentration in vivo is modeled by zero order production (q) and first order loss (k_{met}) constants:

$$dB/dt = q - k_{met}B \quad \text{(Eq. 4)}$$

k_{met} is composed of renal (k_r) and nonrenal (k_{nr}) terms:

$$k_{met} = k_r + k_{nr} \quad \text{(Eq. 5)}$$

At steady state (ss), $dB/dt = 0$, and

$$B_{ss} = q/k_{met} = q/(k_r + k_{nr}) \quad \text{(Eq. 6)}$$

When renal filtration of sTac is changed to α, the fraction of normal glomerular filtration rate (GFR), then the new steady state Tac level, B_{ss}', is increased by the fraction:

$$B_{ss}'/B_{ss} = 1 + (1 - \alpha)/[\alpha + k_r/k_{nr}] \quad \text{(Eq. 7)}$$

$$= 1 + (\beta - 1)/[1 + \beta k_r/k_{nr}] \quad \text{(Eq. 8)}$$

in which β, the serum creatinine, is inversely related to GFR. The filtration ratio is the ratio of Tac relative to creatinine filtered through the glomerulus:

$$FR = k_r * V_d/GFR \quad \text{(Eq. 9)}$$

GFR for mice is ~0.1 ml/min and the plasma volume is ~1 ml, which is taken as the volume of distribution, V_d, during the early time (β-reduced) extrapolation (24).

Experimental Model for Effect of Antibody on Catabolism

Intravenous Bolus. Radiolabeled Tac (B*) or anti-Tac (A*) was administered alone or with excess unlabeled antibody or antigen. Radiolabeled UPC, an isotype-matched, irrelevant mAb, was included as an internal control. Five mice were used in each group. The design of Expt. A2 ensures that antibody will saturate labeled Tac throughout the experiment, but the excess of Tac in Expt. A4 saturates labeled anti-Tac only to 60 h by a two-compartment simulation (not shown). Accordingly, no statistics are reported for A4, which are derived in a more rigorous design in which unlabeled Tac was repeatedly injected intraperitoneally to maintain continuous excess of antigen over antibody. I.p. injection of Tac regenerates the 4–5-h $t_{1/2}$ of the serum and whole body β-phase kinetics after i.v. injection, while avoiding the large α-phase loss that accompanies i.v. dosing. This strategy follows that pursued by Chang et al. (25) to prolong IL2 survival. Tests of plasma confirmed >90% saturation of anti-Tac through the experiment, whereas anti-Tac before administration was >90% bioactive (bindable). Five mice were used in each group.

Expt.	Form	Labeled protein	Labeled protein	Unlabeled protein
A1	B*	^{131}I-Tac (0.3 μg; 10 pmol)	^{125}I-UPC	——
A2	AB*	^{131}I-Tac (0.3 μg; 10 pmol)	^{125}I-UPC	anti-Tac (100 μg; 670 pmol)
A3	A*	^{131}I-anti-Tac (0.15 μg; 1 pmol)	^{125}I-UPC	——
A4	A*B$_2$	^{131}I-anti-Tac (0.15 μg; 1 pmol)	^{125}I-UPC	Tac (100 μg; 4,000 pmol)

Expt.	Form	Labeled protein	Labeled protein	Unlabeled protein, i.p.
A3a	A*	^{131}I-anti-Tac (0.15 μg; 1 pmol)	^{125}I-UPC	——
A4a	A*B$_2$	^{131}I-anti-Tac (0.15 μg; 1 pmol)	^{125}I-UPC	Tac (50 μg; 2,000 pmol)‡

‡Administered every 12–24 h

Continuous infusion. Animals were implanted subcutaneously with pumps secreting ^{131}I Tac (B*), then injected with ^{125}I anti-Tac (A) or nonspecific IgG. Two or three mice were used in each group.

Expt.	Form	Continuously infused Labeled protein	Bolus injected Labeled protein
B1	B*	^{131}I-Tac (2.6 μg; 80 pmol)	^{125}I-UPC (200 μg; 670 pmol)
B2	AB*	^{131}I-Tac (2.6 μg; 80 pmol)	^{125}I-anti-Tac (200 μg; 670 pmol)

Derivation of Equations for Survival Kinetics and Anti-Tac | Tac Interaction

Bolus Intravenous Dosing. The net clearance of anti-Tac (A) is modeled as the sum of the separate first order clearances of the three States of A (1–3) in chemical equilibrium (Schema 2). Clearance of sTac (B) is similarly modeled by three States (2–4), in which two are shared with anti-Tac as complexes and the last is occupied by free sTac. (AB is similarly related to B as shown for AB_2, as indicated by dashed lines.) The interacting kinetics and equilibria were solved numerically (not shown) for the time-dependent concentrations of A, B, AB, and AB_2.

Schema 2.[1]

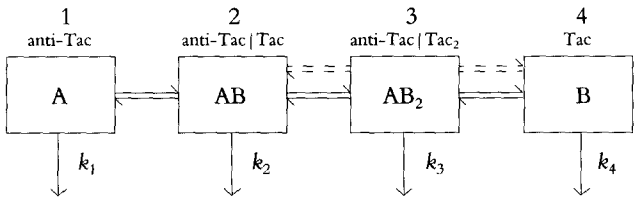

Continuous Infusion and Antigen Steady State. Where antigen is continuously produced, the formulation must include the production rate, q. In the absence of antibody:

$$dB/dt = q - k_4B \quad \text{(Eq. 10)}$$

$$B_{ss} = q/k_4 \quad \text{(Eq. 11)}$$

In the presence of antibody,

$$dB_{tot}/dt = q - k_4B - k_2AB - 2\ k_3AB_2 \quad \text{(Eq. 12)}$$

This is solved numerically as above, from which $B_{tot,ss}$ is derived.

Model Simplifications. When antigen binding does not affect antibody survival, the kinetic model may be reduced from four to two states: State 1: Tac bound and all anti-Tac forms, with a prolonged clearance; State 2: Tac free, with a rapid clearance (Schema 3). This permits simplification of the rate equations

$$dA_{tot}/dt = -k_1\{A + AB + AB_2\} = (-k_1A_{tot}) \quad \text{(Eq. 13)}$$

$$dB_{tot}/dt = -\{k_4\gamma + k_1(1-\gamma)\}B_{tot} = -k'B_{tot} \quad \text{(Eq. 14)}$$

in which $\gamma = B/B_{tot}$ (the fraction of free Tac) and k' is a number-average rate constant that lies between that of antibody (k_1) and free Tac (k_4), biased by the fraction of bound versus free Tac; for large A, $k' = k_1$. Eq. 14 retains the form of a first order differential equation with log-linear plots for γ constant over the experiment. The assumption of equal kinetic constants for Tac (B) and anti-Tac (A) in the same complex (AB or AB_2) is a hypothesis tested in these studies.

Schema 3.

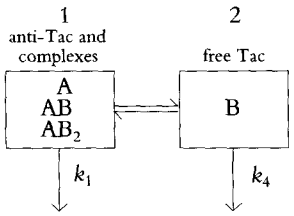

The simplified equations for antigen steady state are similarly:

$$dB_{tot}/dt = q - k'B_{tot} \quad \text{(Eq. 15)}$$

$$B_{tot,ss} = q/k' = (qt'_{1/2}/ln2) \quad \text{(Eq. 16)}$$

For large A, $k' = k_1$, and the new steady state is increased by k_4/k_1, the theoretical maximum. Anticipating results in text, this maximum is k_4/k_2^{Tac} where catabolism of antigen-in-complex is faster than antibody-in-complex.

Results

Shedding of the IL2R α Subunit, Tac

There is no independent secretory mRNA for Tac that could undergo independent regulation (27–29); hence, all sTac is derived from proteolytic cleavage of TM-Tac (9). We therefore wished to know the relation of Tac shedding to TM-Tac expression.

Patients with adult T cell leukemia (ATL) have elevated TM-Tac on their malignant cells, but this expression may increase substantially during culture in vitro that is not seen with normal T cells (30). For the patient of Fig. 1, TM-Tac expression increased progressively over the 4 d period of the assay. Cell number was stable and viability remained ≥90%. Therefore, increased expression in the culture reflected increased expression per cell, which was corroborated on flow cytometry (not shown). The cumulative level of sTac in the supernatant also increased during the period, such that by day 4 it exceeded TM-Tac on cells by a factor of 10 (Fig. 1 *B*), although TM-Tac was itself rapidly increasing over the same period.

Shedding of Tac Is First Order with Respect to Membrane Tac. We consider two general mechanisms of shedding, saturable and nonsaturable. If mechanisms of shedding are saturable—as in a typical Michaelis-Menton enzymic process—an increase in TM-Tac will yield a less-than-proportionate increase in sTac shedding as saturation is approached, yielding finally a zero order process with a fixed, "maximal" rate, although TM-Tac was increasing. If shedding mechanisms are not saturable—as in a spontaneous or autocatalytic process—the rate of shedding should be first order and proportional to TM-Tac. Stated alternately, the fractional shedding rate in a first order process would be constant for all levels of TM-Tac, with an invariant $t_{1/2}$; in a zero order process (or Michaelis-Menton approaching saturation), fractional shedding would decrease with higher TM-Tac with a progressively increasing $t_{1/2}$. This situation, in which the same cells express different levels of TM-Tac over time, presents a special opportunity to distinguish between these models of cellular shedding.

sTac levels for each 24-h period were fit to a model in which sTac production was first order relative to TM-Tac expression (see Materials and Methods). TM-Tac increased almost 40-fold in the example of Fig. 1, from 5,000 molecules/cell to 180,000/cell over 4 d, yet the $t_{1/2}$ was virtually constant for all levels of TM-Tac (Table 1; ATL1/1). Similarly, a survey of donor cell assays in Table 1, including the activated T cells of a normal donor, shows no instance in which increasing TM-Tac to high levels correlates with a prolonged $t_{1/2}$. The relative constancy of $t_{1/2}$ with different TM-Tac expression levels in individual Tac-expressing malignancies and activated T cells is compatible with a first

[1]This formulation should not be confused with classical compartmental analysis. The mouse is treated as a single physical compartment in which A and B move among the different States by a continuous equilibrium. The k values are the microscopic catabolic rate constants for each species. k_4 is the same as k_{met} of Schema 1. The on and off rates for antigen with antibody [26] are rapid relative to the catabolic processes; their explicit representation does not materially alter conclusions, and are therefore omitted. The simulations are available from the authors.

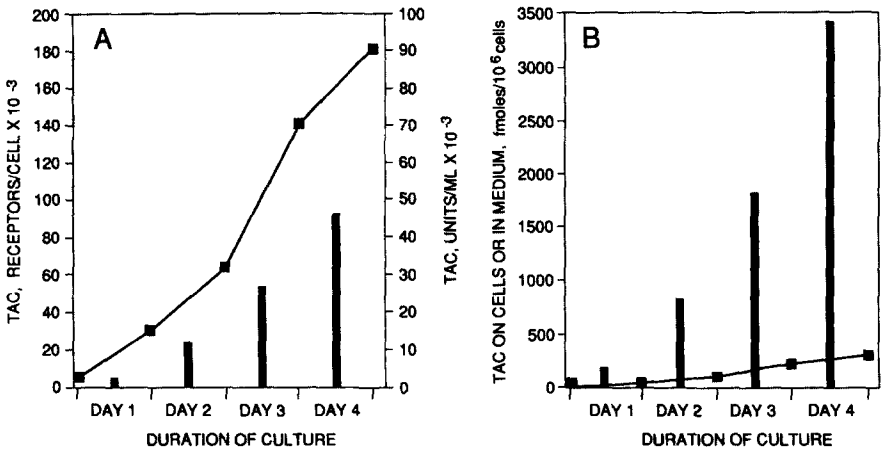

Figure 1. TM-Tac upregulation and high level sTac production by primary ATL cells in culture. Cells were obtained from donor 1 (Table 1). (*A*) Number of TM-Tac per cell and concentration in U/ml of sTac in the culture medium. (*B*) Total moles of Tac which are cell associated or soluble. (—■—) TM-Tac; (*bars*) sTac accumulation between zero time and cell harvesting.

order model. In addition, the same rapid $t_{1/2}$ for Tac shedding is seen with a malignant T cell line of activated phenotype (HuT102) which constitutively expresses high levels of TM-Tac. A zero order or saturable model would have shown proportionately longer $t_{1/2}$ with higher TM-Tac expression, which was not observed. We may therefore exclude any simple zero order model to explain soluble Tac production.

The determinations in Table 1 show a modal $t_{1/2}$ of 2–6 h for Tac shedding that encompasses the malignant T cells from two of six ATL patients, one malignant T cell line, and normal activated T cells. However, individual exceptions were noted, with outliers at the high end where shedding was almost inapparent ($t_{1/2}$ 40–180 h), despite measurable TM-Tac levels, and during late phases of normal T cell activation (Table 1).

When shed in vitro, Tac accumulates as a stable component in the medium. In vivo, however, Tac is subject to the normal catabolic activities of the host, which occupy the remainder of this investigation.

Metabolism of sTac

To estimate the in vivo fate of sTac after it is released from cells, we investigated the pharmacokinetic behavior of a recombinant human sTac protein in mice. Our initial studies examined the serum die-away profile to derive rate and volume constants via compartmental analysis. Tac was rapidly cleared in a two-phase kinetic pattern (Fig. 2),

Table 1. *Shedding $t_{1/2}$ Values Are Not Prolonged by High TM-Tac Levels*

	Cell population studied																	
	ATL1/1																	
Day	Shedding $t_{1/2}$, h	Tac/cell $\times 10^{-3}$	ATL1/2		ATL2		ATL3		ATL4		ATL5		ATL6		ProLL		Hut102		Activated T cell	
0		(5)		(6)		(3)		(7)		(4)		(6)		(9)		(4)				(3)
1	**10.7**	(30)	**6.5**	(33)	**3.4**	(8)	**7.7**	(9)			**18.8**	(14)	**45.0**	(16)	**23.1**	(4)			**3.7**	(90)
2	**6.0**	(63)	**3.2**	(65)	**1.3**	(12)	**8.0**	(19)	**11.3**	(3)	**13.9**	(12)	**190.2**	(26)	**109.7**	(4)	**4.4**	(180)	**3.2**	(74)
3	**6.1**	(141)	**6.2**	(63)	**4.3**	(16)	**6.4**	(22)	**16.2**	(7)	*	(7)	**86.8**	(23)	**86.3**	(3)			**3.2**	(59)
4	**5.6**	(181)	**3.9**	(125)	**3.7**	(17)	**14.4**	(16)	**10.3**	(13)			*	(24)						(49)
5											**8.1**	(3)			**80.5**	(5)			**10.1**	(24)
6																				
7																				
8																			**59.9**	(14)

Primary malignant T cells or T cell line HuT102 were cultured and assayed at various times for TM-Tac and released sTac. $t_{1/2}$ values in hours (**bold**) and TM-Tac $\times$ 10^{-3}/cell (in parentheses) are represented. $t_{1/2}$ values were derived as in Materials and Methods. The two instances for ATL1 represent evaluations before treatment and during a relapse 6 mo later. Too high culture cell number in ATL1/2 exhausted medium by day 3, slowing shedding and Tac upregulation, which both recovered with medium replenishment on day 3 (day 4 data). Activated T cell data were calculated from published data of Jacques et al. [22] using rested T cell blasts that were stimulated at time zero. *Rate constant could not be calculated.

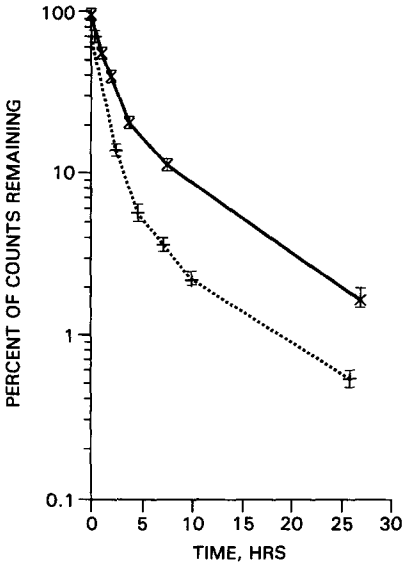

Figure 2. Rapid loss of sTac injected intravascularly. Mice were injected with radiolabeled Tac with blood sampling for the protein bound fraction at indicated times (···+···) and compared with the fractionated (protein-bound) whole body data (—×—) from a further experiment. The unfractionated whole body counts from both studies (not shown) indicated comparability of the experiments. (*Bars*) ±1 SE.

whereas a typical slow catabolism of coadministered IgG was observed (not shown, but see Fig. 4 *B*). The terminal, β-phase of the blood curve parallels the fractionated (protein-associated) whole body curve, as expected (31). The α-phases are not comparable because of key differences in the formulations' treatment of the distribution constants: for blood, the rate of loss is accelerated by extravascular distribution; for whole body, the rate of loss is delayed by extravascular distribution. The derived constants from the venous sampling of two experiments are listed in Table 2.

The elimination rate constant, k_{met}, of 0.49–0.63 h^{-1} corresponds to a catabolic $t_{1/2}$ of 1.1–1.4 h. Intercompartmental transfer rates (k_{ve} and k_{ev}; Schema 1) are relatively directionally unbiased with $t_{1/2}$ values of ~2 h, suggesting passive distributive mechanisms. Two values for steady state volume of distribution relative to plasma volume (V_{ss}/V) are determinable: from the venous sampling curve fit, 2.4–2.6 (Table 2) and from the ratio of area-under-the-curve values (not shown) of the whole body and venous protein curves, 2.2 (Fig. 2). Similar ratios were previously measured for albumin and IgG (32).

Thus, the metabolism of Tac presents a system in which the catabolic rates are faster than the distribution rates, as will be true of many soluble receptors and ligands that are small enough to pass the glomerular filter. This accordingly alters the meaning of α- and β-phase kinetics relative to proteins with longer in vivo survivals. The α-phase kinetics of the whole body and, to a lesser degree, the blood curves are dominated by catabolism, and the β-phase of the blood and whole body curves alike are dominated by distribution kinetics. That is, the β-phase represents sTac that transferred to tissue during the early phase of the experiment which is gradually returning to the vascular-catabolic compartment with a consequent delay in catabolism. It is accordingly noted that neither macroscopic constant adequately represents the true microscopic catabolic rate constant. However, this catabolic constant can be determined as indicated in Table 2.

Extravascular to Intravascular Transport of Tac. Tac-expressing malignant cells or activated T cells are located mainly in the spleen, lymph nodes, skin, and other tissues. Elementary pharmacokinetic principles dictate that catabolism of Tac released into these tissues will be delayed by the time required for Tac to pass from tissue to blood if that tissue does not contribute to the short-term catabolism of Tac. Venous sampling suggested transport to blood with a k_{ev} ~0.3–0.4 h^{-1} and a slightly faster reverse rate (Table 2). To

Table 2. *Kinetic Constants Demonstrating Pattern of Normal Tac Distribution and Catabolism*

		Kinetic constants		Derived $t_{1/2}$ values	
		Expt. 1	Expt. 2	Expt. 1	Expt. 2
		h^{-1}		h	
α	(Macroscopic rate constant)	1.12 (0.17)	1.10 (0.06)	0.62	0.63
β	(Macroscopic rate constant)	0.14 (0.04)	0.14 (0.01)	4.95	4.95
k_{met}	(Metabolic rate constant)	0.63 (0.05)	0.49 (0.02)	1.10	1.41
k_{ve}	(Vascular to extravascular rate)	0.38 (0.10)	0.45 (0.03)	1.82	1.54
k_{ev}	(Extravascular to vascular rate)	0.26 (0.09)	0.32 (0.03)	2.67	2.17
V_{ss}/V	(Normalized distribution volume)	2.6 (0.48)	2.4 (0.10)		

Kinetic constants were derived by two-compartment modeling (Schema 1) as in Materials and Methods. Expt. 1 is represented in Fig. 2; expt. 2 involving nine mice is not shown. Fitting errors are in parentheses. α and β are the macroscopic rate constants. The microscopic constants are k_{met}, the overall metabolic rate constant, and k_{ve} and k_{ev}, the rate constants for transfer from blood to tissue and from tissue to blood. V_{ss}/V is the distribution volume at steady state as a multiple of the plasma volume (the initial volume of distribution).

mimic this in vivo situation more directly, we investigated the peritoneum as an extravascular site for Tac administration.

Fig. 3 shows a comparison of blood and whole body kinetics of animals administered Tac by i.v. or i.p. routes. The blood kinetics after i.v. injection show an α-phase $t_{1/2}$ of 0.6 h, comparable with that of Fig. 2, representing the sum of catabolism and distribution. In contrast, the i.p. injection shows a delayed transfer of radioactivity from the peritoneum to the blood over a period of 2 h and then displays loss kinetics with a $t_{1/2}$ of 4 h that is paralleled in the whole body curves (Fig. 3 *B*). The 4-h $t_{1/2}$ of intraperitoneally injected material is comparable to the 5-h terminal $t_{1/2}$ of the i.v. data of Fig. 2, which was interpreted as the delayed return to blood of sTac that transferred extravascularly. The control IgG transports from peritoneum to blood and then remains stable over the remainder of the experiment. A further comparison of i.p. and s.c. administrations of Tac suggested comparable transfer rates to blood from either of these two extravascular sites (not shown). We conclude that Tac shed into tissues will be transported to the vascular space and catabolized with a combined $t_{1/2}$ for the transport and catabolic processes of about 4–5 h, adding 3–4 h of net delay to the catabolic $t_{1/2}$ of Tac in blood.

Renal Catabolism of Tac. Small proteins such as Bence Jones proteins (Ig L chain monomer [22 kD] and dimer [44 kD]) are cleared primarily by renal mechanisms with a serum $t_{1/2}$ of ~1 h in humans and in mice, which typically parallel humans in the handling of proteins by the kidney (23, 24, 31, 33). Our studies demonstrating rapid clearance of Tac led to our hypothesis of renal catabolism for this ~30kD (33a) glycoprotein as well.

The role of the kidney in catabolism of Tac was assessed by nephrectomy in mice. The ratio of catabolic rates between control and nephrectomized animals indicates the fraction of catabolism attributable to kidney. Ureter ligation inhibits filtration by 11–67% over the first 8 h (34, 35) and provides a setting of moderately reduced GFR. Because whole body sampling represents the sum of vascular and extravascular compartments, the distribution of protein to tissue delays the loss kinetics in contrast to venous sampling in which distribution accelerates loss kinetics. In this setting, the catabolic rate constant is obtained from the initial time kinetics when the system approximates a single, vascular compartment.

As for the venous sampling studies, ^{131}I-Tac was coinjected with ^{125}I-irrelevant IgG as a large protein not normally catabolized in the kidney (Fig. 4). The catabolic rate constants (k_{met}) and time to catabolism of 50% of injected Tac were 0.72 h^{-1} for control mice ($t_{1/2}$ 1.0 h), 0.28 h^{-1} for ureter-ligated mice ($t_{1/2}$ 2.4 h), and 0.07 h^{-1} for nephrectomized mice ($t_{1/2}$ 10 h) (Table 3). These rates indicate that 90% of catabolism is renal with the remaining 10% due to other tissues. In contrast, the concentration of IgG remained high over the study period for normal, ureter-ligated and nephrectomized mice in accord with prior results (23). The catabolic rate constant, k_{met}, represents the sum of renal (k_r) and nonrenal (k_{nr}) terms (Eq. 5). Assigning 0.07 h^{-1} to k_{nr} from the nephrectomy data, we infer a rate constant of 0.72–0.07 = 0.65 h^{-1} for k_r in normal mice. For the ureter-ligated animals, k_r is 0.28–0.07 = 0.21 h^{-1}, indicating a 68% reduction in GFR, which is compatible with expected GFR loss (34, 35). From Eq. 9, we derive a renal filtration ratio of 0.11 for Tac relative to creatinine.

All whole body sTac curves in Fig. 4 *A* show progressive prolongation of survival with time. For the normal animals, this may be explained (above) by the portion of sTac penetrating extravascular tissues during the first 4 h that then diffused back into the blood to gain access to the renal catabolic compartment, as shown previously for L chain dimers

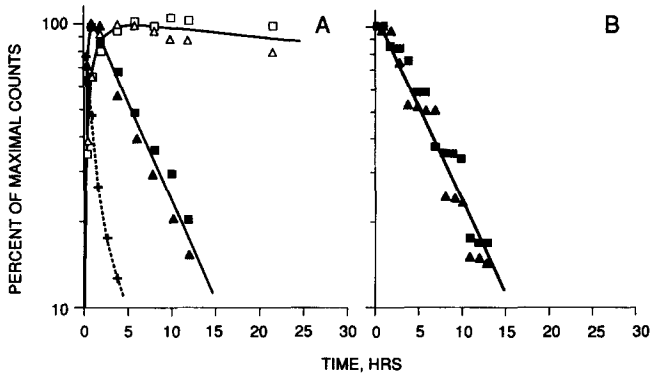

Figure 3. Slower loss of sTac injected intraperitoneally. (*A*) Blood kinetics. A mixture of ^{131}I-Tac (*closed symbols*) and ^{125}I-UPC (*open symbols*) was injected intraperitoneally in two mice (▲, △, mouse 1; ■, □, mouse 2). Superimposed in this graph are the serum loss kinetics from other mice injected with Tac intravenously (···+···). (*B*) Whole body unfractionated loss kinetics of intraperitoneally injected ^{131}I-Tac. Symbols as in *A*. The stair-step effect of whole body loss reflects voiding intervals of the mice; this imposes a lag on the kinetics but does not affect the slope (k).

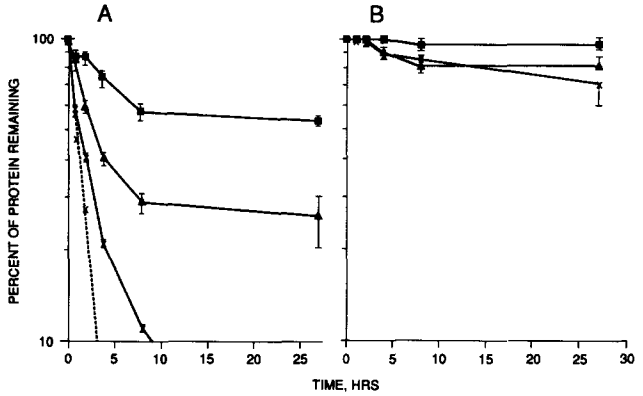

Figure 4. The kidney is the principal site of Tac metabolism. Mice were control (unoperated) or operated with nephrectomy or ureter ligation and administered ^{131}I-Tac plus ^{125}I-UPC, a nonspecific mouse monoclonal IgG. Animals were killed at indicated times and assayed for protein-bound radioactivity in whole body homogenates as in Materials and Methods. Two to five mice were used for each time point. (*Bars*) ±1 SE. (*A*) ^{131}I-Tac, (*B*) ^{125}I-UPC. (■) Nephrectomy; (▲) ureter ligated; (— × —) normal; and (···×···) linearized α-phase of "normals" curve. The linearized α-phase was derived from the full curve of control whole body data (truncated for graphing purposes) by curve stripping; the β phase $t_{1/2}$ was 4 h.

Table 3. *Kinetic Constants Demonstrating Role of Kidney in Tac Metabolism*

	k_{met}	Protein $t_{1/2}$	Percent metabolism due to catabolism	Percent metabolism due to proteinuria
	h^{-1}	h		
Control	0.72 (0.06)	1.0	97–99%	1–3%
Ureter ligated	0.28 (0.03)	2.4	N/A	N/A
Nephrectomy	0.07 (0.01)	10.2	N/A	N/A

The data of Fig. 4 were analyzed by curve stripping to define the α-phase of the control animals, and derived graphically for the two operated sets of animals. In this experimental design, the derived macroscopic α-phase rate constant equals the microscopic metabolic rate constant (k_{met}) (Materials and Methods). *N/A*, not applicable.

(23). These considerations should apply equally to the ureter-ligated animals that retain 30% of GFR, but these intercompartmental rates are less important in the β phase when catabolism is slower. The plateaus after 8 h in ureter-ligated and nephrectomized mice are probably due to uremia-induced suppression of catabolism in these animals, as previously shown (23).

Renal Excretion of Tac. The excretion products after ^{125}I-Tac administration were examined to quantitate the degree of proteinuria. Inasmuch as the tissue-catabolized ^{125}I-Tac will release iodide and iodotyrosine to the kidneys, urinary collection represents the sum of all catabolic products rather than just those generated by the kidney. The spot urine of three normal mice 6 h after injection and the cumulative 48-h collections on a further three animals showed comparable fractions of protein-associated radioactivity (0.7–2.3 and 1.2-3.3%, respectively). The remaining 97–99% was degraded to low molecular weight radioiodine products (Fig. 5), interpreted principally as free iodide (36). Thus, of the sTac entering the blood, 10% is catabolized at external sites and the remaining 90% is filtered through the glomerulus. Of this 90% renal metabolism, 1–3% is due to proteinuria; the remaining portion (87–89%) of Tac passing the glomerular filter is catabolized in the renal tubules (24, 33).

Fig. 6 summarizes the data on the generation and normal catabolism of soluble Tac.

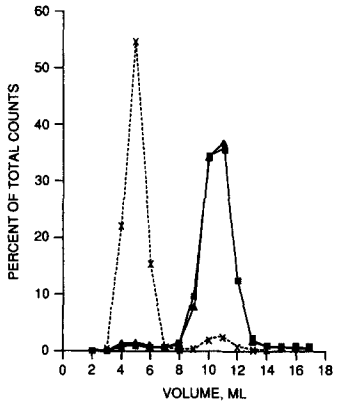

Figure 5. Minor loss of Tac by proteinuria. The urinary products of Tac metabolism were examined by Sephadex G25 chromatography of the cumulative 48-h urine output of two mice after ^{125}I-Tac administration (— ■ —, — ▲ —). As control, the profile of a ^{125}I-sTac preparation with 5% free iodide is shown (···×···).

Antibody Inhibits Tac Catabolism

During antibody therapies, the binding to soluble antigen has the potential to disturb the receptor's normal catabolism. To define the impact of this interaction, two experimental approaches were employed: (*a*) an i.v. bolus injection model to derive catabolic constants, and (*b*) a continuous production model to measure changes in steady state soluble receptor levels.

Bolus Injection: Anti-Tac Binding Prolongs In Vivo Survival of Tac. The survivals of radiolabeled Tac (B*), radiolabeled anti-Tac (A*), and their complexes were examined. Inspection of Schema 4 reveals that only four species can be studied directly: the free forms, B* and A*, and their saturated complexes, AB* and A^*B_2; the crossed forms can only be created in the presence of additional labeled species.

Schema 4.

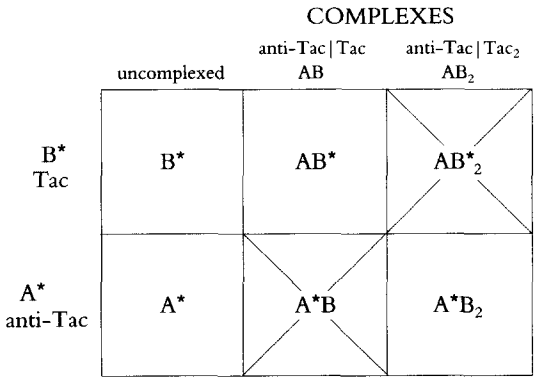

Kinetics analysis of the survival of Tac alone (B*) showed a β $t_{1/2}$ of ~5 h and a catabolic $t_{1/2}$ of 1.4 h (Fig. 7 and Table 4), reflecting the dominance of intercompartmental rate constants previously noted (Fig. 2 and Table 2). The addi-

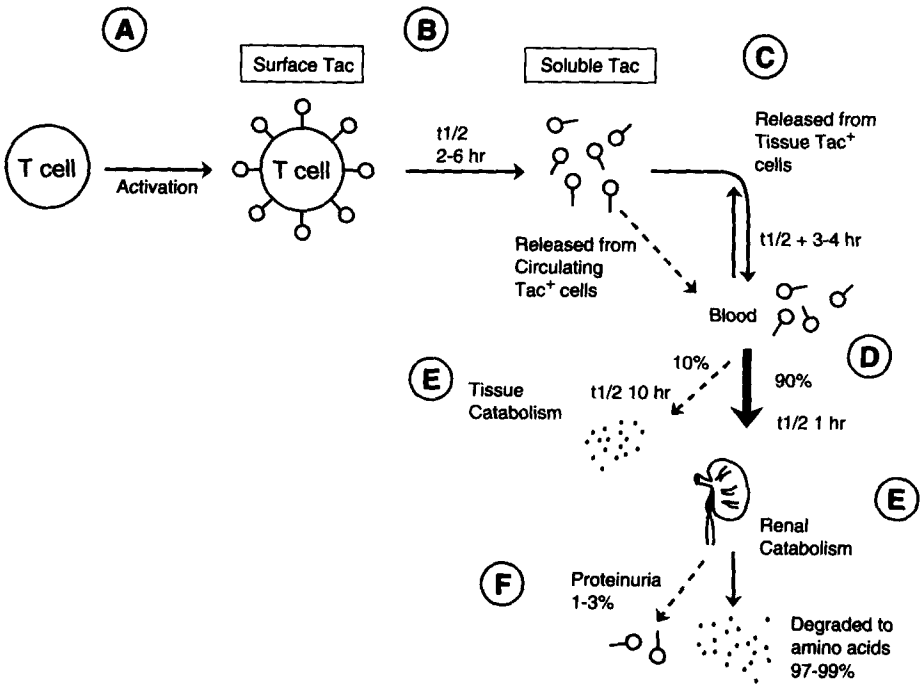

Figure 6. Model of Tac shedding and normal catabolism. (*A*) Expression. TM-Tac is upregulated via nuclear factor-κB-like element interactions in response to activation or viral-induced factors. (*B*) Shedding. Shedding occurs with a modal $t_{1/2}$ of 2–6 h ($k \sim 0.1$–$0.3\ h^{-1}$) after activation or in malignancy. Divergence from this number may be due to dysregulation of coexpressed membrane proteases and/or glycosylation differences. (*C*) Distribution. sTac released in or returning to tissues is governed by bidirectional rate constants of ~0.3–0.4 h^{-1} with a net increase in survival $t_{1/2}$ of +3–4 h over a single (vascular) compartment. (*D*) Filtration. Tac reaching the vascular compartment, or released from circulating cells, is 90% filtered through the glomeruli at ~0.7 ml/h in mice (11% of GFR) and, by extension, ~800 ml/h in humans. (*E*) Catabolism. 10% of catabolism occurs in nonrenal tissues with a $t_{1/2}$ of 10 h (k_{nr} 0.07 h^{-1}), and 90% is mediated by the kidney (k_r 0.65 h^{-1}), yielding a net catabolic $t_{1/2}$ of ~1–1.4 h from blood. After filtration, 97–99% of sTac undergoes tubular resorption and degradation to amino acids with reutilization. (*F*) Excretion. A small (1–3%) fraction of filtered sTac is excreted intact as proteinuria.

tion of anti-Tac antibody increased Tac* (AB*) survival, with a β $t_{1/2}$ of 38 h for Tac in the presence of excess anti-Tac and a catabolic $t_{1/2}$ of 24 h, more than 15-fold above the 1.4-h catabolic $t_{1/2}$ measured for unbound Tac (B*). Anti-Tac antibody (A*) showed a β $t_{1/2}$ of 82 h, with a corresponding catabolic $t_{1/2}$ of 43 h, typical of mAbs in mice. The $t_{1/2}$ for radiolabeled bound Tac (AB*) is significantly different from radiolabeled anti-Tac (A*) ($p < 0.001$).

Because of concerns over the the design of this experiment to maintain excess B over A* beyond 60 h (Expt. A4, Materials and Methods), a more rigorous test was performed, in which antigen excess was maintained via recurrent i.p. Tac (B) dosing (Fig. 8). The new rate of anti-Tac* decline after Tac dosing was not different from that in mice with no antigen administration (p = NS for all comparisons) (Table 5). We conclude that saturation binding with Tac antigen does not alter antibody survival, that is, A^*B_2 survives equal to A*.

An unexpected feature of the data of Fig. 8 was the positive increment of ^{131}I-anti-Tac* radioactivity in the blood after the first Tac dose, which was not seen in the control group. This was observed in each of the five mice in this test, and it was not observed in the nonspecific ^{125}I-IgG control antibody that was coadministered in the same mice (not shown). Different physiologic phenomena may be posited for this observation, but this was not a focus of our study and we did not investigate it further.

These survival data (Tables 4 and 5) present us with a further surprising result. Paradoxically, anti-Tac (A*) and bisaturated anti-Tac complex (A^*B_2) were equal, suggesting no effect of Tac binding on antibody survival, yet the clearance of the monosaturated anti-Tac complex with Tac-labeled (AB*) was significantly faster than either, although it is intermediate structurally between them (Schema 4). Accordingly, the equivalence of the clearance rates of A*, A^*B (presumed, supra) and A^*B_2 versus the apparent faster clearance of AB* suggests a compromise between (*a*) the accelerated clearance of dissociated Tac, and (*b*) the prolonged survival of Tac complexed with antibody. To examine this hypothesis, we modeled the setting in which $k_1 = k_2 = k_3$ and the rate constants k_2 and k_3 apply to both members of each complex (Schema 2). We then tested whether the predicted fraction of free Tac (B*) could explain the accelerated clearance of Tac* in the AB* complex versus anti-Tac (A) in the same complex. The equation for this setting is (Schema 3):

$$dB_{tot}/dt = -\{k_4\gamma + k_1(1-\gamma)\}B_{tot} = k'B_{tot} \qquad \text{(Eq. 14)}$$

At the concentrations of anti-Tac present, $\gamma < 0.001$ (the fraction of free Tac, B/B_{tot}), and the net survival of Tac (k') should have been indistinguishable from that of the antibody (k_1). Yet the survival of Tac-in-complex (Table 4) is only 55% of that predicted. Analysis of the terminal decay phase and steady state levels of Fig. 9 below and other tests not shown likewise demonstrate significantly low fractions (35–45%) of predicted survival and concentrations of sTac by this model. Therefore, we conclude that this hypothesis—that the fraction of Tac that exists dissoci-

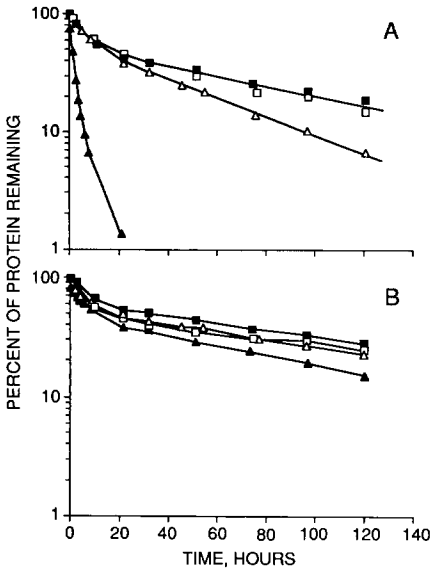

Figure 7. Prolongation of Tac survival in vivo by anti-Tac binding. Samples were prepared and administered intravenously to four groups of animals as in Materials and Methods. (*A*) Blood die-away curves for ^{131}I-Tac* alone, B* (—▲—); Tac* plus excess unlabeled anti-Tac, AB* (—△—); and ^{131}I-anti-Tac*, A* (—■—); anti-Tac* plus excess unlabeled Tac, A^*B_2 (—□—). (*B*) Blood die-away curves for ^{125}I irrelevant IgG (UPC) coadministered in the experiments of *A* with corresponding symbols; that is, ^{125}I-UPC in the experiment with B* (—▲—); in the experiment with AB* (—△—); in the experiment with A* (—■—); and in the experiment with A^*B_2 (—□—). SE not shown, equals 0–3% for all points.

ated in the circulation explains the more rapid net clearance rate—is incompatible with the data and must be rejected. The alternative is that catabolism of Tac-in-complex is genuinely faster than antibody-in-complex. This is considered in the Discussion.

Micropump Infusion: Anti-Tac Increases Steady State Concentrations of Tac in Blood. During T cell activation and malignancy in vivo, sTac is continuously produced by Tac-expressing cells, which are concentrated in extravascular tissues. To model this biologically relevant condition, we observed Tac levels in mice with implanted microosmotic pumps. Similar kinetics and steady state blood levels from s.c. or i.p. implantation (not shown) confirm that the production of Tac in alternative extravascular sites will not be greatly site-sensitive in evaluating metabolism.

To mimic the therapeutic setting, we then examined the impact of specific antibody. 20 h after pump placement, mice were injected intraperitoneally with a large excess of ^{125}I-anti-Tac (A) (Fig. 9). In contrast to the control Tac (B*) infusion, which was already stable at the 20-h time point, the concentration of Tac with anti-Tac injection (AB*) was just approaching plateau at the time of pump expiration after day 7. The blood-soluble Tac level increased 11-fold with anti-Tac antibody during the experiment, and was projected by graphical methods to plateau finally at a 13-fold increase. At no time, however, did Tac reach a concentration that could saturate antibody, which was always at least 100-fold in molar excess. After pump expiration, AB* complex declined with a terminal β $t_{1/2}$ of 41 h that compares with the 38-h β $t_{1/2}$ after bolus injection (Table 4).

These studies indicate that the blood concentration of Tac was increased more than 10-fold by the presence of anti-Tac. This change in concentration occurred in the absence of any alteration in the rate of Tac delivery into the system ("production") and was therefore due solely to suppression of catabolism and prolongation of Tac survival.

Discussion

A wide array of cell surface proteins are present in soluble form in blood that have been assessed for clinical and biological significance. Some, such as B cell IgG, derive from alternately spliced mRNAs that yield the membrane and secreted forms. For all others, the TM protein is shed to generate the soluble form. Phospholipases may be responsible in some instances, but most are thought to be cleaved by membrane-associated proteases (6, 37–40), including at least one phosphoinositol-linked protein (41). Despite the importance of this feature (shedding) and the number of relevant molecules, a recent review concluded that "no convincing candidate for a [shedding protease] has been unequivocally identified and isolated" (6). To our knowledge, this statement remains true. It is notable that the only

Table 4. *Anti-Tac Prolongs Tac Survival*

Form	Description	β $t_{1/2}$	Catabolic rate constant	Catabolic $t_{1/2}$	Difference versus A*
		h	h^{-1}	*h*	
B*	Tac*	4.8 (0.4)	0.485 (0.016) (k_4)	1.43 (0.05)	$p < 0.001$
AB*	Tac* + excess anti-Tac	38 (1)	0.0294 (0.0008) (k_2)	23.6 (0.6)	$p < 0.001$
A*	Anti-Tac*	82 (2)	0.0160 (0.0002) (k_1)	43.1 (0.6)	——

Constants (and fitting errors) were derived from two-compartment analysis of the data of Fig. 7A. A^*B_2, radiolabled anti-Tac saturated with excess cold Tac, is not represented in this table but is separately compared with A* in Table 5. The kinetic constants (k_4, k_2, k_1), are defined in Schema 2. The catabolic constants were compared with anti-Tac (A*) by Student's *t* test.

Table 5. *sTac Does Not Alter Anti-Tac Survival*

Form	Description	$t_{1/2}$ full range	$t_{1/2}$ before injection	$t_{1/2}$ after injection
			(d)	
A^*	Anti-Tac*	5.4 (0.3)	4.5 (1.0)	6.2 (0.8)
A^*B_2	Anti-Tac* + excess sTac	5.5 (0.4)	5.1 (0.4)	5.8 (0.3)
p value		NS	NS	NS

Constants were derived from regression analysis of the data of Fig. 8. The macroscopic β $t_{1/2}$ values (and fitting errors) are expressed in units of days. The full range applies to the approximately linear phase between 1.5 and 6.5 d on the control anti-Tac* (*A**) injection. Because of the positive displacement of the A^*B_2 curve, a full range β was derived as a weighted average of the before injection and after injection averages. The time points before injection are 1.5–3.5 d, and after injection are 3.5–6.5 d. There are no significant differences between the control and experimental slopes by Student's *t* test.

example to date of a defined shedding mechanism is that of FcεR-II, which is autoproteolytic (42).

Like other proteins, the mechanism of Tac shedding is unknown. It proceeds in the absence of serum, is not blocked by several serine protease inhibitors, zinc chelators, or cysteine-reactive agents, and is uninfluenced by the presence or absence of IL2 (9, and R.P. Junghans, unpublished results). The site of Tac cleavage was defined by Robb and Kutny (9) as the Cys^{192}-Leu^{193} bond, for which no specific protease has to our knowledge been described. Mullberg et al. (39) made the cogent observation that the position from the membrane may be more important than the sequence for IL6 receptor shedding, but the strong conservation between mouse and human of a discrete domain surrounding the Tac cleavage site (12/13 = 93%) is reminiscent of the conservation of cleavage motifs for membrane protein processing in paramyxo- and lentiviruses (43) and suggests the sequence is crucial to Tac shedding.

Our two key experimental observations pertinent to mechanism are: (*a*) shedding is nonsaturable over a two-log range of substrate TM-Tac expression; and (*b*) the fractional rate is not uniform across all settings. Accordingly, all models are constrained to appear first order over the range of TM-Tac here, yet must incorporate a potential for interindividual variation in absolute fractional rates of shedding. Both true first order (autocatalytic) and Michaelis-Menton (enzymic) mechanisms can be accommodated, but with significant restrictions to each.

Differences in the shedding rate constant in a first order model may be accommodated by modification of the protein itself, for which role glycosylation is postulated to protect against degradative proteases (44) and is particularly apt as a candidate mechanism. Removal of an O-glycosylation site in transferrin receptor, for example, markedly accelerates release of the soluble form (45). Tac has O-glycosylation sites in proximity to the Cys^{192}-Leu^{193} cleavage site (46), and glycosylation patterns for Tac in normal and ma-

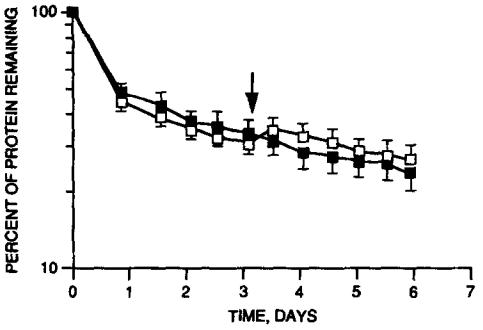

Figure 8. Undisturbed anti-Tac survival in vivo with soluble Tac binding. The experiment was performed as in Materials and Methods, with the first dose of 50 μg of Tac i.p. at 75 h (*arrow*) in the experimental series with repeat dosing every 12–24 h until the end of the experiment. anti-Tac*, A^* (—■—); anti-Tac* plus excess unlabeled Tac, A^*B_2 (—□—). (*Bars*) ±1 SE.

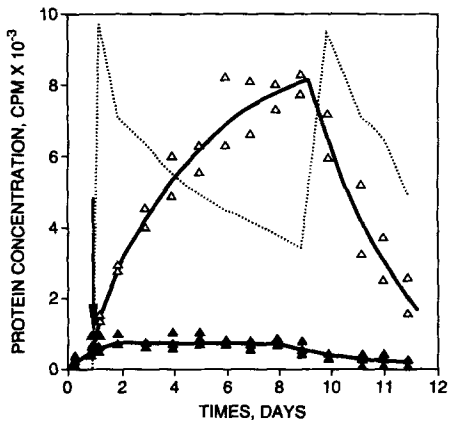

Figure 9. Increased Tac levels with anti-Tac administration in model of constant in vivo antigen production. Pumps (7 d) containing ^{131}I-Tac were inserted subcutaneously (Materials and Methods). A large excess of ^{125}I-anti-Tac or ^{125}I irrelevant IgG (UPC) was given by i.p. bolus at 20 h (*arrow*) as Tac levels approached steady state. Results from two or three mice are pooled in each experiment for graphing. ^{131}I-Tac, B* (—▲—); ^{131}I-Tac plus excess anti-Tac, AB* (—△—). ^{125}I-anti-Tac, A (···), to estimate the anti-Tac excess: the lowest anti-Tac (A) levels were 80 μg/ml plasma or ~500 nM; the highest soluble Tac levels in the AB* mice were 5 nM.

lignant T cells show variation by gel mobilities of extracted proteins (28, 47). Whether this pattern also changes during T cell activation and downregulation of Tac is, to our knowledge, unknown.

On the other hand, this variation in shedding rates is what most suggests a separately regulated protease. If such a "shedding protease" is present, it appears to be membrane bound because (*a*) shedding proceeds in serum-free medium, and (*b*) early and late rates of shedding are constant—medium accumulation of a secreted protease would be expected to progressively accelerate shedding. A recently described matrix metalloenzyme is such a membrane protease (48). The unusual character of the Tac cleavage site and the resistance of Tac shedding to several protease inhibitors argue against a range of nonspecific proteases, but the activity must be widespread, including lymphoid and nonlymphoid cell lines of human and nonhuman origin, since all such cells shed efficiently when transfected with human TM-Tac (29; and R.P. Junghans, unpublished results). "Widespread expression" is expected for an autocatalytic model. Finally, it can be shown that the first order kinetic pattern imposes a high K_m on such a protease, or it implies compensating substrate modification by altered glycosylation at high TM-Tac levels and/or coordinate regulation of the protease. Protein kinase C has been implicated as an activator for a putative shedding protease in one case (37).

Whichever mechanism underlies the shedding process, shedding could have as its normal role to increase receptor release with activation with subsequent return to baseline activity once the activation stimulus is removed. This would promote rapid downregulation of Tac expression and IL-2 responsiveness with withdrawal of the activating stimulus, at a time when maintaining the activated state would be counterproductive to the host.

Once Tac is shed as a soluble protein, it is subject to the catabolic activities of the host. We studied exogenously administered human sTac in a mouse model, which typically parallels humans in metabolic handling of proteins. sTac was rapidly cleared after i.v. injection with a nominal $t_{1/2}$ of 1 h that increased to 10 h in nephrectomized mice. We conclude that Tac is 90% catabolized by the kidney, with a filtration fraction of 0.11, and the remaining 10% of catabolism is accounted for by nonrenal tissues (Fig. 6). After filtration, all protein is either absorbed in the tubules and catabolized to amino acids with reutilization, or excreted as proteinuria (24), documented as 1–3% in our experiments. Extrapolating to humans, with a normal mean serum sTac of 175 U/ml, a creatinine clearance of 180 liters per day, and an 11% of GFR filtration ratio for Tac from our result in mice, we estimate a daily filtration of 3.5×10^6 U of Tac and production (and total metabolism) of 4×10^6 U of Tac (12 μg). Urinary clearance (proteinuria) of sTac in humans was measured at 1.1×10^5 U per 24 h (13), from which we estimate a mean normal proteinuric rate of 3% relative to total catabolism, which corresponds closely with our result in mice (1–3%) and with L chain proteinuria in humans (~1%) (33). In all respects, these data with sTac parallel the metabolic fate of Bence-Jones proteins and isolated L chain in mice and in humans (23, 24, 33). This clearance pattern is likely to be shared by all shed molecules of a size small enough to pass the renal filter (< ~50 kD).

With this picture of normal Tac catabolism, we considered the potential of two settings to perturb this balance. One is the pathologic changes associated with kidney disease; the other is the iatrogenic condition imposed during therapies with antibodies or other antireceptor molecules. The 68% reduction of renal catabolism of Tac with ureter ligation (Fig. 4) is compatible with the impact on GFR in the hours after ligation (34, 35). Reduced catabolism accompanying reduced GFR is predicted to increase plasma levels of endogenously generated sTac, as modeled in Fig. 10. Since the major part of catabolism is kidney dependent, sTac increases roughly with creatinine for low creatinines until nonrenal catabolism becomes a significant portion of the total. Ultimately, in anephric patients on hemodialysis, creatinine is filtered but molecules the size of Tac are not, and all catabolism is nonrenal, predicting plasma levels 11 times normal without any change in the rate of Tac synthesis and release.

In contrast to filtration, tubular dysfunction has no impact on blood levels but only increases the proteinuric fraction concomitant with the decreased tubular protein resorption. Urinary Tac has been used as a measure of Tac expression in malignancy and in allo- and autoimmune settings (10, 13). However, urinary Tac will be dramatically increased in rejection and other renal diseases with a tubular component, for which there is no valid normalization. Given the additional hazards of urinary Tac interpretation relative to serum, with six-fold interindividual variation in proteinuric fractions among human "normals" (13) (threefold in our mice), there is probably no justifiable role for urinary Tac measurements in any setting.

We then examined the effect of antibody binding on the catabolism of Tac, which shares many features with renal failure without the systemic physiologic consequences. The

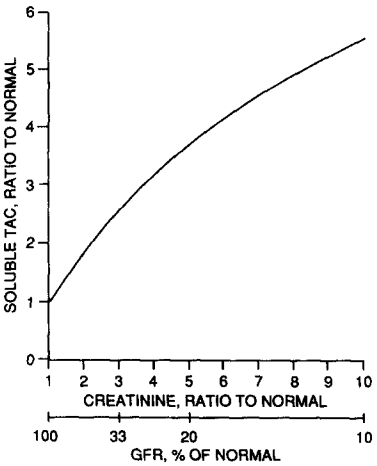

Figure 10. Decreased GFR predicts increased plasma Tac with no change in sTac production. Relative increase in creatinine with normal defined as 1, and fraction of normal GFR represented as the inverse of the relative creatinine. NB: This relation is not applicable in hemodialysis, in which creatinine is filtered and Tac is not.

combination of molecules with different native catabolic rates will have different outcomes, depending upon the mechanisms of clearance. For example, when antidigitoxin Fab antibodies were administered to neutralize digitoxin, the abbreviated survival of the Fab fragment was imposed on the slow $t_{1/2}$ of free drug, leading to a marked acceleration in drug clearance (49). When complete IgG antibodies are themselves the target of antibody-mediated immune reactions, their clearance is usually also greatly accelerated by specific host mechanisms (16). Rapidly catabolized components may alternately have their catabolism delayed by antibody reaction, as first shown for anti-insulin antibodies by Berson and Yalow (50). Similarly, we show that a biologically and clinically important target antigen in soluble form can have its survival markedly prolonged by the interaction with antibody. In contrast, we noted that antibody survival was unaffected by antigen binding.

When antibody elicits antiglobulin responses in vivo, every epitope is repeated twice in IgG (10 times in IgM), and the polyclonality of the response ensures that many epitopes will be targeted, yielding large aggregates that present multivalent Fc to the FcR of the monocyte-macrophage system, and leading to rapid systemic clearance. That anti-Tac survival is unaffected by antigen binding is probably due to the fact that Tac is monomeric and presents a single binding epitope to antibody, which is itself monospecific, thereby avoiding formation of higher aggregates. This should also be generally true for other mAbs targeting monomeric soluble proteins. Furthermore, the size of the antibody was not greatly increased by reaction with antigen. The fully saturated anti-Tac|Tac_2 complex (AB_2) is ~220 versus 160 kD for antibody alone, far below that of other serum proteins such as IgM and complement component C1 (each 900–1,000 kD). The $t_{1/2}$ of IgM in humans is 5 d (31), and greater size alone is insufficient to accelerate clearance.

In contrast, Tac survival increased more than 15-fold with antibody binding, from a nominal 1.4-h catabolic $t_{1/2}$ to 24 h for i.v. injected material. The failure of Tac to pass the glomerular filter when bound to antibody is presumed to be the cause of prolonged Tac survival in the present studies, yielding the equivalent of total renal failure for Tac metabolism. Yet the survival of Tac-in-complex is also much longer than measured for nonrenal catabolism (catabolic $t_{1/2} \sim 10$ h), and antibody evidently protects Tac from this catabolism as well.

To mimic the in vivo setting of human therapies, we applied a continuous production model in mice using implantable microosmotic pumps. As a concomitant of prolonged survival, this model showed increased steady state levels of Tac in the presence of antibody. The steady state concentration (B_{ss}) is a simple function of the rate of production times the catabolic $t_{1/2}$ (not the β $t_{1/2}$; See Materials and Methods):

$$B_{ss} = q/k = q\ t_{1/2}/ln2 \qquad \text{(Eq. 10)}$$

If the $t_{1/2}$ is changed by antibody, then the new steady state for the sum of all B forms, $B'_{tot,ss}$, is related to the former steady state by the ratio of the net $t_{1/2}$ values:

$$B'_{tot,ss}/B_{tot,ss} = t'_{1/2}/t_{1/2} \qquad \text{(Eq. 11)}$$

We measured the $t_{1/2}$ for Tac complexed with anti-Tac as 23.6 h versus a value of 1.4 h for Tac alone (Table 4), predicting a final steady state increase of 16.5-fold. This is comparable with the projected ratio of 13 from our data (Fig. 9), within the uncertainties of this system.

A further consequence of prolonged Tac survival due to any cause (renal failure or antibody binding) will be to alter the normal spatial distributions of Tac in the body. For sTac generated extravascularly, the rapidity of the renal clearance mechanisms in contact with the vascular compartment will generate a steep gradient in the unperturbed setting, with substantially higher levels in the extravascular compartment versus that in blood. With the longer survival, however, this gradient of Tac concentration in vivo is substantially flattened, yielding a marked increase in the normally low physiologic ratio of Tac in serum to Tac body burden.

An unexpected outcome of these studies of Tac metabolism was the apparent faster catabolism of Tac-in-complex versus antibody-in-complex. Our analysis (see Results) eliminated the hypothesis that the shorter $t_{1/2}$ was due to the rapid clearance of the dissociated, free portion of Tac (B^*) in the equilibrium. This left us with the more surprising second alternative: that catabolic activities may attack one part of the anti-Tac|Tac complex, Tac, while sparing the other part, anti-Tac. One speculation may be warranted on the nature of such a process which can selectively "extract" Tac from this high affinity complex. This phenomenon suggests features shared by normal IgG catabolism and intestinal and placental IgG transport (51–53). To explain the acceleration of IgG catabolism with higher serum IgG, Brambell et al. (51) proposed that IgG taken into pinocytic vacuoles is bound to specific IgG receptors (FcR) that redirect its transport to the circulation. Once the putative "protection receptors" are saturated, the remainder of the IgG is subject to unrestricted lysosomal catabolism for a net acceleration at high serum concentrations.

The Brambell hypothesis may be adapted to the present setting. We propose that anti-Tac|Tac complexes are internalized to acidified vesicles as normal IgG. Anti-Tac bound to the protection FcR is returned to circulation, whereas Tac released from the complex in the vesicle is catabolized, thus yielding faster net catabolic rates for circulating antigen-in-complex than antibody-in-complex. That vesicles may be thus topologically "divided" was demonstrated with transferrin and horseradish peroxidase (HRP): both colocalize in early endosomes, but transferrin returns to the surface bound to its receptor whereas HRP proceeds to the late endosomes and lysosomes (54). Endosomes are characterized by reduced pH that is thought to promote ligand–receptor dissociation (54), whereas the relevant Fc–FcR interactions are acid enhanced (53, 55), thereby plausibly enabling IgG recycling to the surface via bound FcR,

free of antigen. Other data suggest that antigen may even be "chewed" out of antibody by endosomal proteases (56). Normal IgG catabolism appears to be widespread, with highest relative activity in liver and spleen (20, 57). Because these sites are rich in cells bearing FcR (including a major nonhematopoietic FcR [55]), this catabolic mechanism has plausibility in the context of these other data. The new feature of this proposal is that it joins these recent in vitro concepts to bulk metabolic observations in whole animals. In any case, the metabolism of Tac in the presence of antibody may introduce a new, slower catabolic route for the antigen which supplants preexisting renal and nonrenal mechanisms. Other monomeric antigen–antibody complexes may be expected to experience similar fates.

It is a necessary consequence of these kinetic studies that prolongation of antigen survival will result in increased steady state sTac levels during antibody therapy unless the mechanisms of Tac production are directly and rapidly suppressed by the therapy itself. We know from other work that Tac production can persist at high levels for at least several days into therapy, even in patients who ultimately undergo complete remission, during which serum Tac levels may increase 10-fold or more (our unpublished results). In the case of anti-Tac, the antibody blocks IL-2 binding by Tac, and higher Tac levels due to antibody complexing will not increase its ability to capture ligand. Moreover, the affinity for IL2 by Tac in isolation is so low (K_a 10^8 M^{-1}) that it would require Tac concentrations of the order of 10 μM to compete 50% with high affinity receptor ($\alpha\beta\gamma$), an inconceivable concentration since the highest antibody concentration in therapy would probably not exceed 0.3 μM (50 μg/ml). (The highest serum sTac level we have observed is 0.05 μM; our unpublished results.) There is accordingly no evidence to suggest an independent regulatory role for the soluble form of this molecule in vitro or in vivo. On the other hand, other cytokines or cytokine receptors to which therapy might be directed could lead to increased biologic activity in vivo if the active site is not also blocked by the antibody, as recently most convincingly shown for anti-IL3, anti-IL4, and anti-IL7 antibodies that capture and stabilize these proteins in active configurations (58).

The role of sTac and other soluble molecules as a surrogate for body burden of tumor or activated T cells can be interpreted in the context of these results. Among ATL patients, there is a general correspondence between disease volume and sTac levels (our unpublished results), as also observed for hairy cell leukemia, another Tac-expressing malignancies (15). Higher sTac levels should correlate with more shedding, but where individuals differ in Tac expression or shedding rate, as noted here, this correlation weakens at the level of estimating numbers of Tac-expressing cells. Donor 1 in Table 1 underwent remission during her treatment with antibody directed at TM-Tac on the surface of her malignant cells. Subsequently, she experienced a relapse of her disease, at which time her cells exhibited a nearly identical pattern of Tac expression and shedding. For this individual, the in vitro results suggest that serum sTac could reasonably be used as a measure of her disease. sTac may thus be useful as a serum marker for many patients in the same sense that elevated CEA concentrations are a marker for recurrence in colon cancer and other malignancies, but in which individuals are known to differ in the relative expression of the marker (59).

Although the plasma level of the soluble form of Tac and other cell surface molecules is a reasonable correlate of physiologic condition or disease expression, its use must be tempered with knowledge of the biology of the protein. We showed that antibody binding markedly inhibits the metabolism of sTac with a corresponding increase in the serum concentration. In addition, as is true for other small molecules, Tac is catabolized chiefly by the kidney. Thus, it is concluded that serum concentrations of soluble antigen in renal failure or during antibody therapy cannot be used as a surrogate measure of tumor burden or T cell activation because receptor levels will both increase and differentially redistribute as a consequence of prolonged survival, in the absence of changes in soluble antigen production.

We thank Mr. Donald Dobbs for his excellent assistance in the animal surgeries and related procedures. We also thank Ms. Shilpa Mhatre, and Drs. Xiang-yang Tan, Gang Zheng, and Gillian Kingsbury for their assistance. We gratefully acknowledge supply of human Tac protein from Dr. John Hakimi of Hoffmann-La Roche, Inc. We also thank Dr. Diane Mould of Hoffmann-La Roche, Inc. for introducing one of us (R.P. Junghans) to pcNONLIN, for advice on aspects of its application, and for early review of the manuscript; and we thank Hoffmann-La Roche, Inc. for providing a purchase donation of the pcNONLIN software. We also thank Drs. Clark Anderson, Ira Mellman, and Victor Ghetie for their comments on our data regarding differential catabolism mechanisms; and Drs. Patricio Silva and Robert Stanton for discussions on the renal implications of these studies.

This work was supported in part by grants to R.P. Junghans from the Milheim Foundation for Cancer Research and a Clinical Oncology Career Development Award from the American Cancer Society.

Address correspondence to: Dr. R.P. Junghans, New England Deaconess Hospital, 99 Brookline Avenue, Room 301, Boston, MA 02215.

Received for publication 9 August 1995; and in revised form 6 December 1995.

Note added in proof: The receptors for IgG protection (FcRp) [51,53] and intestinal transport (FcRn) [52,53,55], both described by Brambell, were recently shown to be identical using mice knocked-out for the receptor light chain (Junghans, R.P. and C.L. Anderson, manuscript submitted for publication). In such mice, IgG protection and differential catabolism were both lost, yielding clearance of antibody- and antigen-in-complex at the same accelerated rate as albumin. This confirms the central role of the FcRp to the differential catabolism mechanism, as postulated in this article.

References

1. Fernandez-Botran, R. 1991. Soluble cytokine receptors: their role in immunoregulation. *FASEB (Fed. Am. Soc. Exp. Biol.) J.* 5:2567–2574.
2. Gearing, A.J.H., and W. Newman. 1993. Circulating adhesion molecules in disease. *Immunol Today.* 14:506–509.
3. Schwartz, M.K. 1993. Cancer markers. *In* Cancer: Principles and Practice of Oncology. 4th ed. V.T. Devita, S. Hellman, and S.A. Rosenberg, editors. Lippincott, Philadelphia. 531–542.
4. Arend, W.R. 1995. Inhibiting the effects of cytokines in human disease. *Adv. Intern. Med.* 40:365–394.
5. Junghans, R.P., G. Sgouros, and D.B. Scheinberg. 1996. Antibody-based immunotherapies in cancer. *In* Cancer Chemotherapy and Biotherapy: Principles and Practice. B.A. Chabner and D.L. Longo, eds. Lippincott-Raven Publ., Philadelphia. 655–689.
6. Ehlers, M.R.W., and J.F. Riordan. 1991. Membrane proteins with soluble counterparts: role of proteolysis in the release of transmembrane proteins. *Biochemistry.* 30:10065–10074.
7. Waldmann, T.A., I.H. Pastan, O.A. Gansow and R.P. Junghans. 1992. The multichain interleukin-2 receptor: a target for immunotherapy. *Ann. Intern. Med.* 116:148–160.
8. Greene, W.C., W.J. Leonard, J.M. Depper, D.L. Nelson, and T.A. Waldmann. 1986. The human interleukin-2 receptor: normal and abnormal expression in T cells and in leukemias induced by the human T-lymphotropic retroviruses. *Ann. Intern. Med.* 105:560–572.
9. Robb, R.J., and R.M. Kutny. 1987. Structure-function relationships for the IL2-receptor system. *J. Immunol.* 139:855–862.
10. Simpson, M.A., P.N. Madras, A.J. Cornaby, T. Etienne, R.A. Dempsey, G.H. Clowes, and A.P. Monaco. 1989. Sequential determinations of urinary cytology and plasma and urinary lymphokines in the management of renal allograft recipients. *Transplantation (Baltimore).* 47:218–223.
11. Lawrence, E.C., V.A. Holland, J.B. Young, and N.T. Windsor. 1989. Dynamic changes in soluble interleukin-2 receptor levels after lung or heart-lung transplantation. *Am. Rev. Respir. Dis.* 140:789–796.
12. Semenzato, G., L.M. Bambara, D. Biasi, A. Frigo, F. Vinante, B. Zuppini, L. Trentin, C. Feruglio, M. Chilosi, and G. Pizzolo. 1988. Increased serum levels of soluble interleukin-2 receptor in patients with systemic lupus erythematosus and rheumatoid arthritis. *J. Clin. Immunol.* 8:447–452.
13. Marcon, L., M.E. Fritz, C.C. Kurman, J.C. Jensen, and D.L. Nelson. 1988. Soluble Tac peptide is present in the urine of normal individuals and at elevated levels in patients with adult T cell leukemia (ATL). *Clin. Exp. Immunol.* 73:29–33.
14. Rubin, L.A., G.S. Hekzema, D.L. Nelson, W.C. Greene, and G. Jay. 1987. Reconstitution of a functional interleukin 2 receptor in a nonlymphoid cell. *J. Immunol.* 139:2355–2360.
15. Ambrosetti, A., G. Semenzato, M. Prior, M. Chilosi, F. Vinante, C. Vincenzi, R. Zanotti, L. Trentin, A. Portuese, F. Menestrina, et al. 1989. Serum levels of soluble interleukin-2 receptor in hairy cell leukemia: a reliable marker of neoplastic bulk. *Br. J. Haematol.* 73:181–186.
16. Meeker, T.C., D.G. Maloney, R.A. Miller, K. Thielmans, R. Warnke, and R. Levy. 1985. A clinical trial of anti-idiotype therapy for B cell malignancy. *Blood.* 65:1349–1363.
17. Schulz, G., D.A. Cheresh, N.M. Varki, A. Yu, L.K. Staffileno, and R.A. Reisfeld. 1984. Detection of ganglioside GD2 in tumor tissues and sera of neuroblastoma patients. *Cancer Res.* 44:5914–5920.
18. Sela, B.-A., D. Iliopoulos, D. Ghuerry, D. Herlyn, and H. Koprowski. 1989. Levels of disialogangliosides in sera of melanoma patients monitored by sensitive thin layer chromatography and immunostaining. *J. Natl. Cancer Inst.* 81:1489–1492.
19. Sharkey, R.M., D.M. Goldenberg, H. Goldenberg, R.E. Lee, C. Ballance, K.D. Pawly, D. Varga, and H.J. Hansen. 1990. Murine monoclonal antibodies against carcinoembryonic antigen; immunological, pharmacokinetic, and targeting properties in humans. *Cancer Res.* 50:2823–2831.
20. Junghans, R.P., D. Dobbs, M.W. Brechbiel, S. Mirzadeh, A.A. Raubitschek, O.A. Gansow, and T.A. Waldmann. 1993. Pharmacokinetics and bioactivity of DOTA-Bismuth conjugated anti-Tac antibody for alpha emitter (^{212}Bi) radioimmunotherapy. *Cancer Res.* 53:5683–5689.
21. Nelson, D.L. 1986. Expression of a soluble form of the interleukin-2 receptor in normal and neoplastic states. The human interleukin-2 receptor: normal and abnormal expression in cells and in leukemias induced by the human T-lymphotropic retroviruses. *Ann. Intern. Med.* 105:560–572.
22. Jacques, Y., B. LeMauff, F. Boeffard, A. Godard, and J.P. Soulillou. 1987. A soluble interleukin 2 receptor produced by a normal alloreactive human T cell clone binds interleukin 2 with low affinity. *J. Immunol.* 139:2308-2316.
23. Wochner, R.D., W. Strober, and T.A. Waldmann. 1967. The role of the kidney in the catabolism of Bence Jones proteins and immunoglobulin fragments. *J. Exp. Med.* 126:207–221.
24. Mogielnicki, P.R., T.A. Waldmann, and W. Strober. 1971. Renal handling of molecular weight proteins. I. L-chain metabolism in experimental renal disease. *J. Clin. Invest.* 50:901–909.
25. Chang, A.E., C.L. Hyatt, and S.A. Rosenberg. 1984. Systemic administration of recombinant human interleukin 2 in mice. *J. Biol. Response Modif.* 3:561–572.
26. Depper, J.M., W.J. Leonard, M. Kronke, P.D. Noguchi, R.E. Cunningham, T.A. Waldmann, and W.C. Greene. 1984. Regulation of interleukin 2 receptor expression: effects of phorbal diester, phospholipase C, and reexposure to lectin or antigen. *J. Immunol.* 133:3054–3061.
27. Leonard, W.J., J.M. Depper, G.R. Crabtree, S. Rudikoff, J. Pumphrey, R.J. Robb, M. Kronke, P.B. Svetlik, N.J. Peffer, T.A. Waldmann, and W.C. Greene. 1984. Molecular cloning

and expression of cDNAs for the human interleukin-2 receptor. *Nature (Lond.).* 311:626–631.
28. Leonard, W.J., M. Kronke, N.J. Peffer, J.M. Depper, and W.C. Greene. 1985. Interleukin-2 receptor gene expression in normal human T lymphocytes. *Proc. Natl. Acad. Sci. USA.* 82:6281–6285.
29. Cullen, B.R., F.J. Podlaski, N.J. Peffer, J.B. Hosking, and W.C. Greene. 1988. Sequence requirements for ligand binding and cell surface expression of the Tac antigen, a human interleukin-2 receptor. *J. Biol. Chem.* 263:4900–4906.
30. Uchiyama, T., T. Hori, M. Tsudo, Y. Wano, H. Umadome, S. Tamori, J. Yodoi, M. Maeda, H. Sawami, and H. Uchino. 1985. Interleukin-2 receptor (Tac antigen) expressed on adult T cell leukemia cells. *J. Clin. Invest.* 76:446–453.
31. Waldmann, T.A., and W. Strober. 1969. Metabolism of immunoglobulins. *Prog. Allergy.* 13:1–110.
32. Humphrey, J.H., and J.L. Fahey. 1961. The metabolism of normal plasma proteins and gamma-myeloma protein in mice bearing plasma-cell tumors. *J. Clin. Invest.* 40:1696-1705.
33. Waldmann, T.A., W. Strober, and P.R. Mogielnicki. 1972. The renal handling of low molecular weight proteins. II. Disorders of serum protein catabolism in patients with tubular proteinuria, the nephrotic syndrome, or uremia. *J. Clin. Invest.* 51:2162-2174.
33a. Junghans, R.P., A.L. Stone, and M.S. Lewis. 1996. Biophysical characterization of a recombinant soluble interleukin 2 receptor (Tac): evidence for a monomeric structure. *J. Biol. Chem.* In press.
34. Dal Canton, A., R. Stanziale, A. Corradi, E. Vittorio, A. Migone, and L. Migone. 1977. Effects of acute ureteral obstruction on glomerular hemodynamics in rat kidney. *Kidney Int.* 12:403–411.
35. Harris, R.H., and J.M. Gill. 1981. Changes in glomerular filtration rate during complete ureteral obstruction in rats. *Kidney Int.* 19:603–608.
36. Lewellan, C.G., M. Berman, and J.E. Rall. 1959. Studies of iodoalbumin metabolism. I. A mathmatical approach to the kinetics. *J. Clin. Invest.* 38:66–87.
37. Harrison, D., J.H. Phillips, and L.L. Lanier. 1991. Involvement of a metalloproteinase in spontaneous and phorbol ester–induced release of natural killer cell-associated FcγRIII (CD16-II). *J. Immunol.* 147:3459–3465.
38. Gearing, A.J.H., P. Beckett, M. Christodoulou, M. Churchill, J. Clements, A.H. Davidson, A.H. Drummond, R. Gilbert, J.L. Gordon, T.M. Leber. 1994. Processing of tumour necrosis factor-α precursor by metalloproteinases. *Nature (Lond.).* 370:555–557.
39. Mullberg, J., W. Oberthur, F. Lottspeich, E. Mehl, E. Dittrich, L. Graeve, P.C. Heinrich, and S. Rose-John. 1994. The soluble human IL6 receptor: mutational characterization of the proteolytic cleavage site. *J. Immunol.* 152:4958–4968.
40. Zhang, L., and B.B. Aggarwal. 1994. Role of sulfhydryl groups in induction of cell surface down-modulation and shedding of extracellular domain of human TNF receptors in human histiocytic lymphoma U937 cells. *J. Immunol.* 153: 3745–3754.
41. Bazil, V. and J.L. Strominger. 1991. Shedding as a mechanism of down-modulation of CD14 on stimulated human monocytes. *J. Immunol.* 147:1567–1574.
42. Letellier, M., T. Nakajima, G. Pulido-Cejudo, H. Hofstetter, and G. Delepesse. 1990. Mechanism of formation of human IgE-binding factors (soluble CD23): III. Evidence for a receptor (FcεRII)-associated proteolytic activity. *J. Exp. Med.* 172:693–700.
43. Morrison, T.G. 1988. Structure, function and intracellular processing of paramyxovirus membrane proteins. *Virus Res.* 10:113–136.
44. Paulson, J.C. 1990. Glycoproteins: what are the sugar chains for? *In* Proteins: Form and Function. R.A. Bradshaw and M. Purton, eds. Elsevier Trends Journals, Cambridge. p. 272–276.
45. Rutledge. E.A., B.J. Root, J.J. Lucas, and C.A. Enns. 1994. Elimination of O-linked glycosylation site at Thr 104 results in the generation of a soluble human transferrin receptor. *Blood.* 83:580–586.
46. Miedel, M.C., J.O. Hulmes, D.V. Weber, P. Bailon, and Y.E. Pan. 1988. Structural analysis of recombinant soluble human interleukin-2 receptor. *Biochem. Biophys. Res. Commun.* 154:372–379.
47. Wano, Y., T. Uchiyama, J. Yodoi, and H. Uchino. 1985. Biosynthetic processing of human interleukin-2 receptor (Tac antigen). *Microbiol. Immunol.* 29:451–466.
48. Sato, H., T. Takino, Y. Okada, J. Cao, A. Shinagawa, E. Yamamoto, and M. Seiki. 1994. A matrix metalloproteinase expressed on the surface of invasive tumour cells. *Nature (Lond.)* 370:61–65.
49. Ochs, H.R., and T.W. Smith. 1977. Reversal of advanced digitoxin toxicity and modification of pharmacokinetics by specific antibodies and Fab fragments. *J. Clin. Invest.* 60: 1303–1313.
50. Berson, S.A., R.S. Yalow, A. Bauman, M.A. Rothschild, and K. Newerly. 1956. Insulin-^{131}I metabolism in human subjects: demonstration of insulin binding globulin in the circulation of insulin-treated subjects. *J. Clin. Invest.* 35:170–190.
51. Brambell, F.W.R., W.A. Hemmings, and I.G. Morris. 1964. A theoretical model of γ-globulin catabolism. *Nature (Lond.).* 203:1352-1355.
52. Brambell, F.W.R. 1966. The transmission of immunity from mother to young and the catabolism of immunoglobulins. *Lancet.* 2:1087–1093.
53. Waldmann, T.A., and E.A. Jones. 1977. The role of cell-surface receptors in the transport and catabolism of immunoglobulins. *In* Protein Turnover, *CIBA Found. Symp.* 9:5–18.
54. Schmid, S.L., R. Fuchs, P. Male, and I. Mellman. 1988. Two distinct subpopulations of endosomes involved in membrane recycling and transport to lysosomes. *Cell.* 52:73–83.
55. Story, C.M., J.E. Mikulska, and N.E. Simister. 1994. A major histocompatibility complex class I-like Fc receptor cloned from human placenta: possible role in transfer of immunoglobulin G from mother to fetus. *J. Exp. Med.* 180:2377–2381.
56. West, M.A., J.M. Lucoca, and C. Watts. 1994. Antigen processing and class II MHC peptide-loading compartments in human B-lymphoblastoid cells. *Nature (Lond.).* 369:147–149.
57. Henderson, L.A., J.W. Baynes, and S.R. Thorpe. 1982. Identification of sites of IgG catabolism in the rat. *Arch. Biochem. Biophys.* 215:1–11.
58. Finkelman, F.D., K.B. Madden, S.C. Morris, J.M. Holmes, N. Boiani, I.M. Katona, and C.R. Maliszewski. 1993. Anticytokine antibodies as carrier proteins. *J. Immunol.* 151:1235–1244.
59. Goldenberg, D.M., A. Neville, A. Carter, V.L. Go, E.D. Holyoke, K.J. Isselbacher, P.S. Schein, and M. Schwartz. 1981. CEA (carcinoembryonic antigen): Its role as a marker in the management of cancer. *J. Cancer Res. Clin. Oncol.* 101: 239–242.